

**Table 26.** Selected bond lengths (Å) and angles(°) for Ni<sup>2+</sup> cross-bridged ligand complexes

(i) For Ni(Me <sub>2</sub> B14N4)(acac) <sup>+</sup>			
Ni(1)-O(21)	2.017(2)	Ni(1)-N(8)	2.111(2)
Ni(1)-O(22)	2.018(2)	Ni(1)-N(11)	2.160(2)
Ni(1)-N(1)	2.107(2)	Ni(1)-N(4)	2.187(2)
O(21)-Ni(1)-O(22)	90.90(9)	N(1)-Ni(1)-N(11)	91.09(9)
O(21)-Ni(1)-N(1)	173.40(9)	N(8)-Ni(1)-N(11)	84.84(9)
O(22)-Ni(1)-N(1)	92.75(9)	O(21)-Ni(1)-N(4)	89.65(9)
O(21)-Ni(1)-N(8)	91.73(9)	O(22)-Ni(1)-N(4)	93.21(9)
O(22)-Ni(1)-N(8)	174.70(9)	N(1)-Ni(1)-N(4)	84.66(9)
N(1)-Ni(1)-N(8)	85.07(9)	N(8)-Ni(1)-N(4)	91.41(9)
O(21)-Ni(1)-N(11)	94.38(9)	N(11)-Ni(1)-N(4)	174.56(10)
O(22)-Ni(1)-N(11)	90.38(9)		
(ii) For Ni(Me <sub>2</sub> B12N4)(acac) <sup>+</sup>			
Ni(1)-O(23)	2.015(3)	Ni(1)-N(11)	2.063(3)
Ni(1)-O(26)	2.023(3)	Ni(1)-N(14)	2.142(3)
Ni(1)-N(17)	2.059(3)	Ni(1)-N(110)	2.149(3)
O(23)-Ni(1)-O(26)	89.93(12)	N(17)-Ni(1)-N(14)	84.90(13)
O(23)-Ni(1)-N(17)	177.11(12)	N(11)-Ni(1)-N(14)	82.18(13)
O(26)-Ni(1)-N(17)	92.64(12)	O(23)-Ni(1)-N(110)	96.85(12)
O(23)-Ni(1)-N(11)	91.96(13)	O(26)-Ni(1)-N(110)	95.03(12)
O(26)-Ni(1)-N(11)	178.05(13)	N(17)-Ni(1)-N(110)	81.61(13)
N(17)-Ni(1)-N(11)	85.46(13)	N(11)-Ni(1)-N(110)	84.29(13)
O(23)-Ni(1)-N(14)	96.06(12)	N(14)-Ni(1)-N(110)	161.58(13)
O(26)-Ni(1)-N(14)	98.08(12)		
(iii) For Ni(Me <sub>2</sub> B14N4)(OH <sub>2</sub> ) <sub>2</sub> <sup>2+</sup>			
Ni(1)-O(1)	2.0909(13)	Ni(1)-O(2)	2.1071(12)
Ni(1)-N(8)	2.0921(13)	Ni(1)-N(4)	2.1509(14)
Ni(1)-N(1)	2.1035(13)	Ni(1)-N(11)	2.1581(13)
O(1)-Ni(1)-N(8)	94.68(5)	N(1)-Ni(1)-N(4)	85.24(6)
O(1)-Ni(1)-N(1)	172.18(6)	O(2)-Ni(1)-N(4)	96.32(5)
N(8)-Ni(1)-N(1)	86.16(5)	O(1)-Ni(1)-N(11)	96.81(5)
O(1)-Ni(1)-O(2)	84.36(5)	N(8)-Ni(1)-N(11)	85.56(5)
N(8)-Ni(1)-O(2)	172.05(5)	N(1)-Ni(1)-N(11)	91.01(5)
N(1)-Ni(1)-O(2)	95.87(5)	O(2)-Ni(1)-N(11)	86.71(5)
O(1)-Ni(1)-N(4)	86.97(5)	N(4)-Ni(1)-N(11)	175.39(5)
N(8)-Ni(1)-N(4)	91.51(5)		

of the analogous Cu<sup>2+</sup>, Mn<sup>2+</sup>, Fe<sup>2+</sup>, and Co<sup>2+</sup> complexes (*vide supra*). First, the size of the ring system dictates the distortion of the octahedra. The 14-membered ring in B14N4 enfolds the metal ion more fully than does the 12-membered ring in B12N4. The N<sub>ax</sub>-M-N<sub>ax</sub> bond angle for Ni(B14N4)(acac)<sup>+</sup> is 174.56(10)°, and for Ni(B14N4)(OH<sub>2</sub>)<sub>2</sub><sup>2+</sup> it is 175.39(5)°, while for Ni(B12N4)(acac)<sup>+</sup>, it is only 161.58(13)°. The smaller angle for the smaller macrobicyclic

demonstrates how the metal ion is less engulfed in the ligand cavity.

A second broad observation is that the smaller Ni<sup>2+</sup> ion is more fully surrounded by both macrobicycles than are the larger Mn<sup>2+</sup>, Fe<sup>2+</sup>, and Co<sup>2+</sup> ions but less so than is Cu<sup>2+</sup>. **Table 27** summarizes the smooth change in N<sub>ax</sub>-M-N<sub>ax</sub> bond angles as a function of the radius of the pseudo octahedral ion. The chelating acac

**Table 27.** Comparison of bond angles of cross-bridged ligand complexes with respect to metal ion

Metal Ion	H.S. 6-Coordinate Ionic Radius	Me <sub>2</sub> B14N4		Me <sub>2</sub> B12N4	
		N <sub>ax</sub> -M-N <sub>ax</sub>	N <sub>eq</sub> -M-N <sub>eq</sub>	N <sub>ax</sub> -M-N <sub>ax</sub>	N <sub>eq</sub> -M-N <sub>eq</sub>
Mn <sup>2+</sup>	97	158.0(2)	75.6(2)	144.0(2)	74.1(2)
Fe <sup>2+</sup>	92	161.88(5)	78.36(5)	145.78(7)	77.31(7)
Co <sup>2+</sup>	88.5	172.4(2)	81.11(13)	149.81(9)	80.86(8)
<sup>‡</sup> Cu <sup>2+</sup>	87	-----	-----	164.85(13)	83.92(14)
<sup>¶</sup> Ni <sup>2+</sup>	83	175.39(5)	86.16(5)	-----	-----
*Ni <sup>2+</sup>	83	174.56(10)	85.07(9)	161.58(13)	85.46(13)
Cu <sup>2+</sup>	79	175.16(13)	85.30(12)	-----	-----
<sup>‡</sup> Cu <sup>2+</sup> complex is Cu(L)(MeCN) <sub>2</sub> <sup>2+</sup> <sup>¶</sup> Ni <sup>2+</sup> complex is Ni(L)(OH <sub>2</sub> ) <sub>2</sub> <sup>2+</sup> (vide supra) *Ni <sup>2+</sup> complexes are Ni(L)(acac) <sup>+</sup> (vide supra) Ionic Radius is for 5-coord Cu <sup>2+</sup> . Complex is Cu(L)Cl <sup>+</sup>					

ligand or two aqua ligands may influence this trend since most of the structures of other metal ions involve MCl<sub>2</sub> complexes, although little deviation from the expected trend is observed except in the N<sub>eq</sub>-Ni-N<sub>eq</sub> angle of the complex of B12N4, where this angle is larger than expected, and for Ni(B14N4)(OH<sub>2</sub>)<sub>2</sub><sup>2+</sup>, whose bond angles are larger than those of the related copper(II) complexes. The electron density of the hard oxygen donor and/or the steric bulk associated with the acac chelate may influence the bond angles as compared to the larger, softer, monodentate chloride ligands present in the other complexes. The chlorides probably take up more space than water molecules, allowing Ni<sup>2+</sup> to sink more deeply into the cavity of the bicyclic ligand in the diaquo complex than would otherwise be expected. Although it is unclear whether water or chloride is bound to nickel (in the cases where water is

included in the formula) in the bulk solids, the non-acac complexes will be referred to as chloro complexes for simplicity.

It is interesting that the rather bulky acac ligand has no steric difficulty binding  $\text{Ni}^{2+}$  in these complexes. Previously discussed studies with iron and manganese complexes of these same ligands demonstrate that the N-methyl groups prohibit dimerization, even under oxidizing conditions known to be favorable for formation of species of the types  $\text{Fe-O-Fe}^{182}$  or  $\text{Mn-(O)}_2\text{-Mn}^{183}$ . Significantly, replacement of the methyl groups by H results in facile dimerization of both the iron and manganese complexes of these otherwise identical ligands under mild oxidizing conditions (*vide supra*). The present structures reveal that steric prevention of dimerization must occur as a result of the fact that two such complexes, when dimerized in pseudo octahedral geometries, would place the methyl groups from both ligands in approximately the same position. However, steric bulk in the plane orthogonal to the  $\text{N}_{\text{ax}}\text{-M-N}_{\text{ax}}$  plane, as in the present acac examples, is not sterically precluded by the N-methyl groups. Discussions of in-plane versus out-of-plane steric bulk have appeared elsewhere.<sup>196</sup>

*Electronic Structure.* The magnetic moments of the three complexes  $\text{NiLCl}_2$  where  $\text{L} = \text{B14N4}$ ,  $\text{B13N4}$ , and  $\text{B12N4}$  fall into a normal range for high spin, octahedral  $d^8 \text{Ni}^{2+}$  complexes.<sup>190</sup> The values are:  $\mu_{\text{eff}} = 3.09$  for  $\text{Ni(B14N4)Cl}_2$ ,  $\mu_{\text{eff}} = 3.19$  for  $\text{Ni(B13N4)Cl}_2$ , and  $\mu_{\text{eff}} = 3.19$  for  $\text{Ni(B12N4)Cl}_2$ . The magnetic moment of the  $\text{Ni}^{2+}$  complex with  $\text{B14N4Me}_6$  was quite high however,  $\mu_{\text{eff}} = 3.51$ . This value is out of the range for a normal octahedral complex but is acceptable for five coordinate complexes of this ion,<sup>190,197</sup> and along with the previously discussed steric demands of this ligand, led to the assumption that the geometry of  $[\text{Ni(B14N4Me}_6\text{)Cl}]\text{Cl}$ , like the other complexes of this ligand, is five coordinate.

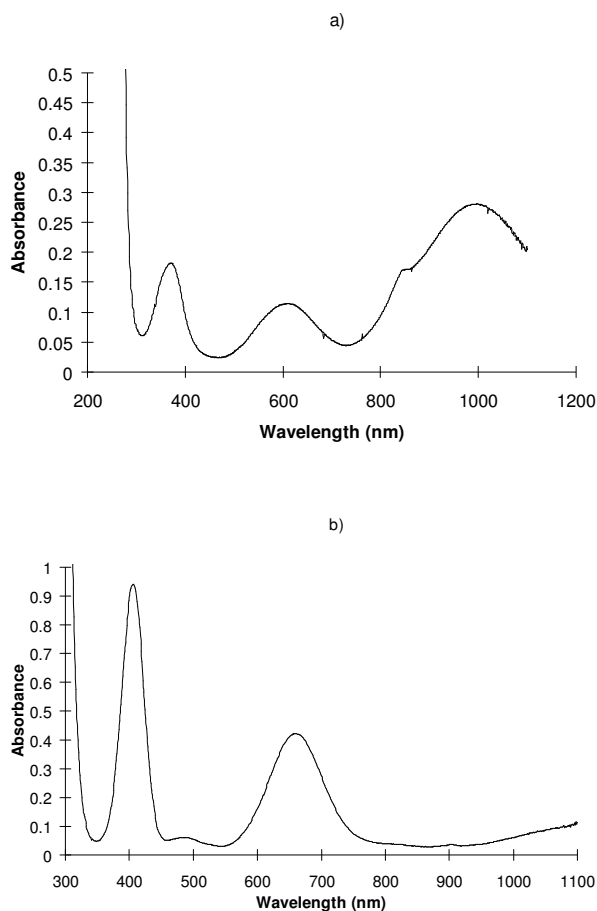


**Figure 85.** Electronic spectra of a) Ni(Me<sub>2</sub>B13N4)Cl<sub>2</sub> and b) Ni(Me<sub>2</sub>B14N4Me<sub>6</sub>)Cl<sup>+</sup> 0.01 M in MeCN

**Table 28.** Electronic spectra of Ni<sup>2+</sup> complexes in MeCN

Complex	Absorbance[nm] (Extinction Coefficient [M <sup>-1</sup> cm <sup>-1</sup> ])
Ni(Me <sub>2</sub> B14N4)Cl <sub>2</sub>	393(18), 484(8), 979(13)
Ni(Me <sub>2</sub> B13N4)Cl <sub>2</sub>	373(14), 601(9), 994(20)
Ni(Me <sub>2</sub> B12N4)Cl <sub>2</sub>	370(18), 608(11), 1016(28)
Ni(Me <sub>2</sub> B14N4Me <sub>6</sub> )Cl <sup>+</sup>	406(94), 660(42)

The electronic spectra of the four chloride complexes reinforce our assumption of the coordination geometries. NiLCl<sub>2</sub> (L = B14N4, B13N4, and B12N4) all exhibit classic octahedral Ni<sup>2+</sup> electronic spectra, with three major absorptions in the range of 300-1100 nm, as exemplified by the spectrum of Ni(B13N4)Cl<sub>2</sub> in acetonitrile (**Figure 85**). The absorbances are collected in **Table 28**. However, [Ni(B14N4Me<sub>6</sub>)Cl]PF<sub>6</sub> displays a much different spectrum that is consistent with five-coordination.<sup>191a,197</sup>

Literature examples of trigonal bipyramidal Ni<sup>2+</sup> complexes with N<sub>4</sub>Cl donor sets most closely resemble that of [Ni(B14N4Me<sub>6</sub>)Cl]PF<sub>6</sub>. These complexes have only two major absorptions in the 300-1100 nm range, with extinction

coefficients larger than normal for octahedral Ni<sup>2+</sup>. One band is usually centered from 700-800 nm with an extinction coefficient approximately twice that of the other, which is centered from 400-500 nm.<sup>191a,197</sup> Clearly, the spectrum of Ni(B14N4Me<sub>6</sub>)Cl<sup>+</sup> better approximates known examples of this geometry than it does the classic octahedral spectra of the other three complexes.

The electronic spectra of octahedral Ni<sup>2+</sup> complexes are particularly useful for the determination of the ligand field strengths of ligands.<sup>178</sup>  $\Delta_o$  is directly determined by the energy of the lowest energy absorption band. For the three octahedral dichloro complexes this gives the following results:  $\Delta_o = 10,215 \text{ cm}^{-1}$  for Ni(B14N4)Cl<sub>2</sub>,  $\Delta_o = 10,060 \text{ cm}^{-1}$  for Ni(B13N4)Cl<sub>2</sub>, and  $\Delta_o = 9,843 \text{ cm}^{-1}$  for Ni(B12N4)Cl<sub>2</sub>. A trend is evident; the larger macrobicyclic exerts a larger ligand field strength on Ni<sup>2+</sup>, probably because it forms a less distorted octahedron as noted above in the N<sub>ax</sub>-M-N<sub>ax</sub> bond angles of the Ni(B14N4)(acac)<sup>+</sup> and Ni(B12N4)(acac)<sup>+</sup> crystal structures. Comparisons of these values with those of Ni<sup>2+</sup> complexes with some unbridged tetraazamacrocycles is enlightening. The value for *cis*-Ni(13N4)Cl<sub>2</sub> was determined<sup>198</sup> as  $\Delta_o = 11,111 \text{ cm}^{-1}$  while that of *cis*-Ni(TACD)(NO<sub>3</sub>)<sub>2</sub> is  $\Delta_o = 9,756 \text{ cm}^{-1}$  (TACD = 1,4,7,10-tetrabenzyl-1,4,7,10-tetraazacyclododecane).<sup>197b</sup> These values indicate the ligand field strengths of the ethylene cross-bridged tetraazamacrocycles are very similar to those of unbridged analogues which bind in a similar *cis* fashion. The value Dq<sub>xy</sub> is the measure of ligand field strength analogous to  $\Delta_o$  for tetragonally distorted complexes,<sup>199</sup> the usual geometry associated with tetraazamacrocycles that chelate in a planar fashion. Values for Dq<sub>xy</sub> are consistently much higher than those of  $\Delta_o$  for *cis*-binding of analogous ligands and this is also true of the ethylene cross-bridged ligands. For example Dq<sub>xy</sub> = 14,870 cm<sup>-1</sup> for *trans*-Ni(14N4)Cl<sub>2</sub>,<sup>199</sup> which is much higher than  $\Delta_o$  of Ni(B14N4)Cl<sub>2</sub> given above. These *trans* complexes are also generally low spin, which is explained by the fact that the smaller low spin ion fits the planar macrocycle's cavity better. In the case of the cross-bridged ligands, planar

coordination and the very strong ligand field strength associated is topologically prevented, producing high spin Ni<sup>2+</sup> complexes of the typical lower ligand field strengths associated with *cis*-tetraazamacrocycles.

**Table 29.** Molar Conductance of Ni<sup>2+</sup> cross-bridged ligand complexes

Complex	Molar Conductance			
	H <sub>2</sub> O	MeCN	DMF	MeNO <sub>2</sub>
Ni(Me <sub>2</sub> B14N4)Cl <sub>2</sub> · 2H <sub>2</sub> O	185	127	61	32
Ni(Me <sub>2</sub> B13N4)Cl <sub>2</sub> · H <sub>2</sub> O	213	134	64	32
Ni(Me <sub>2</sub> B12N4)Cl <sub>2</sub> · 0.5H <sub>2</sub> O	205	176	62	21
[Ni(Me <sub>2</sub> B14N4Me <sub>6</sub> )Cl]PF <sub>6</sub>	171	123	70	80
1:1	118-131	120-160	65-90	75-95
2:1	235-273	220-300	130-170	150-180
Ref. 166 used for theoretical conductance values				

*Solution Properties.* The results of conductance experiments on the chloride complexes (**Table 29**) reflect the ease with which the chloride ligands may be replaced by solvent. The ionization (displacement of chloride by solvent) of these complexes in solution correlates with the dielectric constant and coordinating ability of the solvent. In the low dielectric non-coordinating solvent, nitromethane, the six coordinate complexes approach the behavior of non-electrolytes revealing that the chlorides remain bound and indicating that the structure of the complexes in solution is probably six coordinate and pseudo octahedral, as in the solid state. In contrast, the five coordinate complex [Ni(B14N4Me<sub>6</sub>)Cl]PF<sub>6</sub> behaves, as expected, as a 1:1 electrolyte but without dissociation of the one bound chloride ligand. In coordinating solvents with slightly higher dielectric constants, like acetonitrile and DMF, all four complexes behave as 1:1 electrolytes which implies that solvent has displaced one chloride ligand from the coordination sphere of the six coordinate complexes. In

water, behavior intermediate between a 1:1 and 2:1 electrolyte is observed for all of the complexes, indicating that the last chloride ligand has only been partially replaced by water molecules in both the five and six coordinate complexes. For those cases of bulk solid samples where water is present in the composition, it has not been definitively determined whether water or chloride is bound to the nickel. For that reason, it may be more appropriate to discuss the conductivity measurements in terms of chloride replacing water, rather than solvent replacing chloride in some cases. In either event, the conductivity data indicates how many, and in which solvents, chloride is bound to nickel in solution.

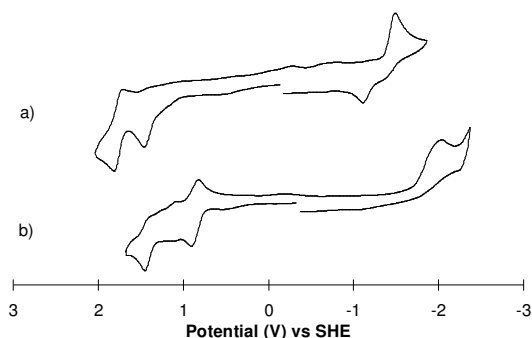


**Figure 86.** Cyclic voltammograms of a)  $\text{Ni}(\text{Me}_2\text{B14N4Me}_6)\text{Cl}^+$  and  $\text{Ni}(\text{Me}_2\text{B12N4})\text{Cl}_2$  in MeCN

The cyclic voltammograms of (a)  $[\text{Ni}(\text{B14N4Me}_6)\text{Cl}]\text{PF}_6$  and (b)  $\text{Ni}(\text{B12N4})\text{Cl}_2$  in MeCN are shown in **Figure 86**. The latter is representative of all three six coordinate chloro complexes. The redox potentials and peak separations of all four chloro complexes can be found in **Table 30**. These rigid ligands stabilize a range of oxidation states for nickel,

**Table 30.** Electrochemistry of  $\text{Ni}^{2+}$  cross-bridged ligand complexes in MeCN

Complex	$E_{\text{red}}$ (V) $\text{Ni}^{2+}/\text{Ni}^+$	$E_{1/2}$ (V) $\text{Ni}^{3+}/\text{Ni}^{2+}$	$(E_a - E_c)$ (mV) $\text{Ni}^{3+}/\text{Ni}^{2+}$	$E_{\text{ox}}$ (V)
$\text{Ni}(\text{Me}_2\text{B14N4})\text{Cl}_2 \cdot 2\text{H}_2\text{O}$	-1.894	+0.991	154	+1.325
$\text{Ni}(\text{Me}_2\text{B13N4})\text{Cl}_2 \cdot \text{H}_2\text{O}$	-1.991	+1.001	77	+1.323
$\text{Ni}(\text{Me}_2\text{B12N4})\text{Cl}_2 \cdot 0.5\text{H}_2\text{O}$	-2.036	+0.863	68	+1.450
$[\text{Ni}(\text{Me}_2\text{B14N4Me}_6)\text{Cl}]\text{PF}_6$	-1.301	+1.760 ( $E_{\text{ox}}$ )	106	+1.492

from  $\text{Ni}^+$  to  $\text{Ni}^{3+}$  as shown by the reversible oxidation, assigned as the  $\text{Ni}^{3+/2+}$  cycle, and irreversible reduction to  $\text{Ni}^+$ , observed for their  $\text{Ni}^{2+}$  complexes. Also of note is the ring size effect from the 14-membered B14N4 through the 12-membered B12N4. The smallest ring complex (L = B12N4) is much easier to oxidize, which may be explained simply on the basis of metal ion size; the smaller cavity more greatly stabilizes the smaller oxidized metal ion. Conversely, the larger ligands favor the larger, lower valent metal ion which is demonstrated in the easier reduction of the complexes of the larger macrobicyclic ligands. The more difficultly oxidized complexes of B14N4 contain a metal ion more completely enclosed by the macrobicyclic cavity and more removed from the solvent, as shown in the  $\text{N}_{\text{ax}}-\text{M}-\text{N}_{\text{ax}}$  and  $\text{N}_{\text{eq}}-\text{M}-\text{N}_{\text{eq}}$  bond angles (*vide supra*).

The presence of a second, irreversible oxidation for all four complexes is clear, but its origin has not been assigned. The sequence of the reversible  $\text{Ni}^{3+/2+}$  wave followed by the second irreversible oxidation is the same for all three octahedral complexes, while this order is reversed in the voltammogram of  $[\text{Ni}(\text{B14N4Me}_6)\text{Cl}]\text{PF}_6$ . The probable source of the second oxidation process is the irreversible oxidation of bound chloride ligand. Since its potential depends on complex, it is unlikely to involve free chloride.

The striking features of the voltammogram for  $[\text{Ni}(\text{B14N4Me}_6)\text{Cl}]\text{PF}_6$  are its much higher potential for the  $\text{Ni}^{3+/2+}$  couple and the much milder potential for its irreversible reduction to  $\text{Ni}^+$  compared to the three six-coordinate complexes. The much milder reduction of  $[\text{Ni}(\text{B14N4Me}_6)\text{Cl}]\text{PF}_6$  is probably due to the preference of  $\text{Ni}^+$ , a  $d^9$  ion, for five coordination. This reduction is the only one exhibiting a return oxidation, although it is displaced by some 380 mV. We surmise that loss of  $\text{Cl}^-$  by the reduced  $\text{Ni}^+$  accounts for the lack of reversibility here and in the other complexes.  $[\text{Ni}(\text{B14N4Me}_6)\text{Cl}]\text{PF}_6$  must be more difficult to oxidize as a result of its unique geometry as well.  $\text{Ni}^{3+}$  is apparently less well stabilized by the five coordinate

trigonal bipyramidal geometry than by the pseudo octahedral geometries allowed by the other ligands.

In summary, reported above are the synthesis of Ni<sup>2+</sup> complexes of the cross-bridged macrobicyclic ligands B14N4, B13N4, B12N4, and B14N4Me<sub>6</sub> overcoming their proton-sponge nature by reducing the activity of protons in the reaction mixture. Using these simple, but topologically constrained ligands, high spin five and six coordinate complexes have been produced where unbridged tetraazamacrocycles generally produce square planar low spin species. Magnetic and spectroscopic measurements on the chloro complexes show the ligands to have relatively small ligand field strengths, due to the *cis* orientation forced by the ethylene cross-bridge. These measurements also reveal that the coordination spheres of the divalent metal complexes with B14N4, B13N4, and B12N4 are comparable and may be described as six coordinate pseudo octahedra, but the complex of B14N4Me<sub>6</sub> has been characterized as five coordinate with only one bound chloride as a result of ligand steric effects. X-ray crystal structures of Ni(B14N4)(acac)<sup>+</sup>, Ni(B12N4)(acac)<sup>+</sup>, and Ni(B14N4)(OH<sub>2</sub>)<sub>2</sub><sup>2+</sup> confirm the octahedral geometry for these complexes and provide data for comparison with previous structures of these ligands complexed to other metal ions. The smaller ring B12N4 is more distorted in its pseudo octahedral acac complex because the Ni<sup>2+</sup> metal ion is a bit larger than would be ideal for occupancy, whereas the Ni(B14N4)(acac)<sup>+</sup> complex is less distorted from the octahedral ideal because of its larger cavity and better fit for Ni<sup>2+</sup>. This trend is reflected in the electrode potentials of the chloro complexes. The extent to which counter ions (Cl<sup>-</sup>) are dissociated in the chloro complexes increases with the dielectric constant of the solvent resulting in their nearly complete replacement by solvent in water, which produces the two labile *cis* sites needed for many types of catalysis.<sup>27</sup> These Ni<sup>2+</sup> complexes exhibit readily detectable +3 and +1 oxidation states in acetonitrile. Such stabilization of multiple oxidation states is again necessary for various catalytic

cycles. The derivatives of the larger rings are harder to oxidize, which can be traced to a better size match between the larger ring and the larger divalent ions and the smaller rings with the smaller trivalent ions. The coordination geometry uniqueness of the complex with  $B14N4Me_6$  is readily apparent in its electrochemistry as well as its magnetic and spectroscopic properties.

### **Miscellaneous Observations**

During the study of cross-bridged tetraazamacrocycle coordination chemistry, various observations were made that were not necessarily appropriate to discuss as a part of the chapters above. These observations are presented for completeness, below.

### **X-Ray Crystal Structure Determination of *trans*-Dioxocyclam (1,4,8,11-tetraazacyclotetradecane-5,12-dione) and its $Ni^{2+}$ Complex**

Macrocyclic ligands containing amide groups have been greatly exploited recently for transition metal coordination because they share properties with both oligopeptides and the more common polyamine macrocycles.<sup>200</sup> Particular emphasis has been placed on these ligands for use in transition metal oxidation catalysts, because the inherent negative charge of the bound, deprotonated ligand can stabilize high oxidation states of transition metal ions.<sup>200,201</sup> The above studies concerned with the design of aqueous transition metal oxidation catalysts have focussed on the use of intramolecularly cross-bridged tetraazamacrocycles to produce kinetically stable complexes (*vide supra*). The *trans* dioxocyclam ligand 1,4,8,11-tetraazacyclotetradecane-5,12-dione, *trans*-14N4O<sub>2</sub> has recently been shown to be effectively *trans* diprotected for bridging reactions that produce cross-bridged ligands.<sup>87</sup> Cross-bridging such a bis-amide ligand might produce exceptional kinetic stability as well as stabilization of high valent forms of the resulting transition metal complexes. Towards that goal, the coordination chemistry of the unbridged *trans*-

14N4O<sub>2</sub> was briefly explored in order to compare it with the cross-bridged analogues under study by others. Here reported is the crystal structure of *trans*-14N4O<sub>2</sub> and its Ni<sup>2+</sup> complex and further characterization of the latter, including its electrochemical properties.

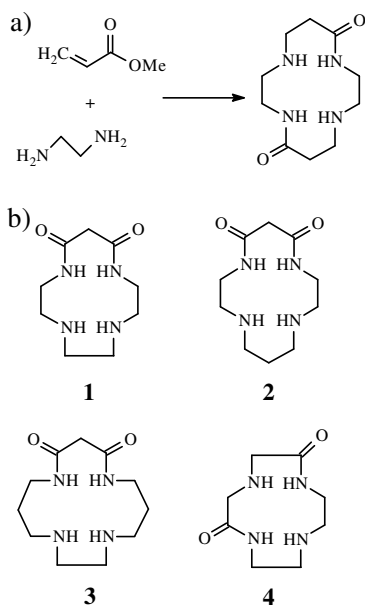


**Figure 87.** Synthesis of *trans*-14N4O<sub>2</sub> (a) and b) structures of related ligands

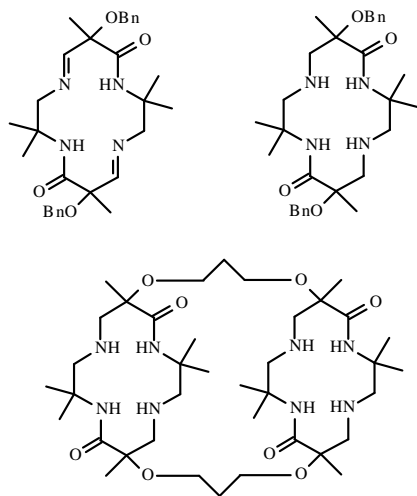


**Figure 88.** Highly substituted *trans*-dioxocyclams known to complex Ni<sup>2+</sup>

The ligand *trans*-14N4O<sub>2</sub> (**Figure 87a**) is a structural isomer of the extensively studied *cis*-dioxocyclam, one of a family of dioxomacrocycles studied by Kimura.<sup>200</sup> The synthesis of the present ligand is quite simple, it being the product of a Michael addition involving ethylenediamine and methyl acrylate.<sup>88</sup> This ligand has been known for nearly fifteen years, yet no work on its transition metal complexes has been published, to our knowledge. However, a few extensively substituted analogues with the same *trans*-dioxo configuration have been synthesized by a much different method, and their Ni<sup>2+</sup> complexes, have been reported (**Figure 88**).<sup>202,203</sup>

In the present case, the ligand *trans*-14N4O<sub>2</sub> was prepared according to the literature procedure.<sup>88</sup> Crystals suitable for X-ray diffraction studies were grown by the slow diffusion of ether into an acetonitrile solution of the ligand. A representation of the crystal structure of *trans*-14N4O<sub>2</sub> · 2H<sub>2</sub>O is shown in

**Figure 89a.** Two molecules of lattice water

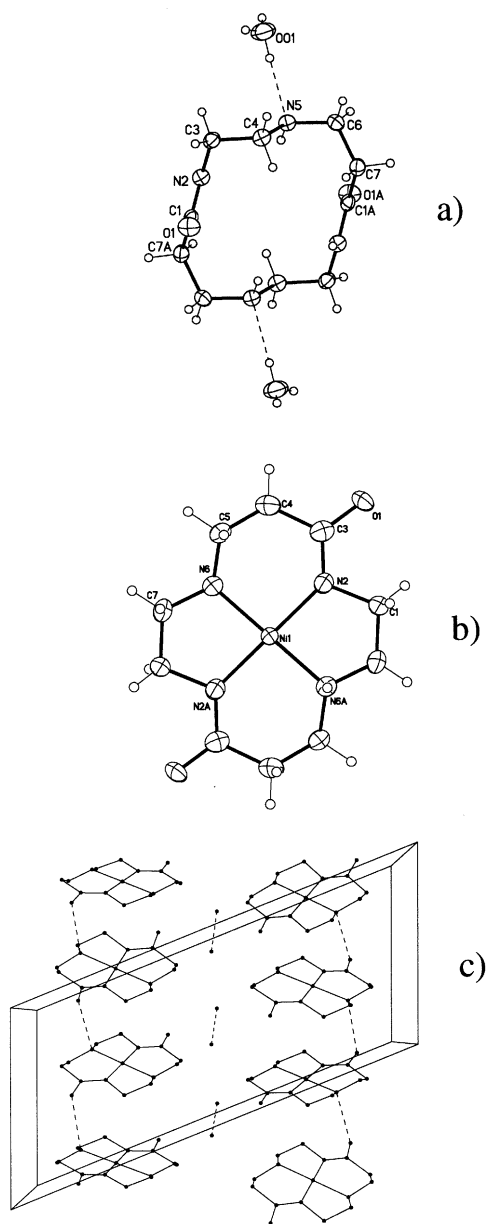


**Figure 89.** Molecular structures of a) *trans*-14N4O<sub>2</sub> and b) Ni(*trans*-14N4O<sub>2</sub>H<sub>2</sub>) along with its crystal packing diagram (c)

were located in the structure, and each is hydrogen bonded to a secondary amine nitrogens of the macrocycle ring. These water molecules have one hydrogen that is disordered between two equivalent positions; the lattice water H-atoms were located and refined in the structure solution. The conformation of the ligand is very similar to that of a hexa C-substituted bis-imine *trans*-dioxocyclam structure previously published,<sup>202</sup> in that the amine nitrogen lone pairs are directed away from the center of the macrocycle. In the present case, hydrogen bonds to the lattice water help stabilize this conformation. The amide functional groups have their carbonyl oxygens on opposite faces of the ring; the amide hydrogens are also directed to opposite faces.

Complexation of *trans*-14N4O<sub>2</sub> with Ni<sup>2+</sup> was achieved by the *in situ* deprotonation of the two amide nitrogens with KH in DMF to produce

amidate donors, followed by the addition of anhydrous NiCl<sub>2</sub> to the DMF solution.

The neutral complex, as well as the KCl biproduct, is insoluble in the DMF reaction

solvent and can be collected by filtration as a mixture of solids. However, once the crude product has been obtained, it can be purified by simply washing the KCl and residual DMF away with water. Some product dissolves in the water washings, but most reprecipitates upon standing. A final filtration and washing with water gives the analytically pure product as a monohydrate. Crystals of the dihydrate suitable for X-ray diffraction studies were obtained by the slow evaporation of the solvent from a methanol solution of the complex. The neutral complex has very limited solubility in most common solvents. Useful concentrations could only be obtained in water and methanol, in both of which, the complex behaves as a nonelectrolyte.

Representations of the crystal structure of Ni(*trans*-14N4O<sub>2</sub>H<sub>2</sub>) · 2H<sub>2</sub>O are shown in **Figure 89b-c**. The Ni<sup>2+</sup> ion is found in a square planar geometry at the center of the bis-amidate macrocycle. A major conformational change occurs as the ligand binds the metal ion, directing all nitrogen lone pairs into the center of the ring and placing the four nitrogen atoms essentially coplanar with Ni<sup>2+</sup>. The metrical parameters for this structure are: Ni(1)-N(2) = Ni(1)-N(2A) = 1.894(5) Å, Ni(1)-N(6) = Ni(1)-Ni(6A) = 1.902(5) Å, N(2)-Ni(1)-N(2A) = N(6)-Ni(1)-N(6A) = 180.0°, N(2)-Ni(1)-N(6) = N(2A)-Ni(1)-N(6A) = 93.9(2)°, N(2)-Ni(1)-N(6A) = N(2A)-Ni(1)-N(6) = 86.1(2)°. The N-Ni-N angles where the nitrogens are separated by an ethylene chain, are smaller by about 8° than these angles where the nitrogens are separated by a trimethylene chain (86.1° vs 93.9°). Yet, the overall symmetry of the complex is high, with linear *trans* N-Ni-N bond angles. The result is a compression of the square plane into a slightly rectangular geometry. The Ni-N(amide) bonds are slightly shorter than the Ni-N(amine) bonds, 1.894(5) Å to 1.902(5) Å, respectively, as might be expected due to the increased charge attraction between the amidate nitrogens and the cation. This bond length difference is about twice that found in the Ni<sup>2+</sup> complex of the related octa-C-substituted ligand having the same size and amide placement (**Figure 87**), where the bond distances are 1.915 Å for Ni-N(amine) and 1.911 Å for Ni-

N(amide).<sup>203</sup> Steric interactions between the ring substituents may explain why this literature example has approximately 0.01 Å longer Ni-N bond lengths than in the present, unsubstituted example. **Figure 89c** shows the interesting hydrogen bonding interaction between adjacent molecules of Ni(*trans*-14N4O<sub>2</sub>H<sub>2</sub>) in the solid state. Each bound ligand is involved in two hydrogen bonds: one secondary amine of each ligand is the H-bond donor to a neighboring ligand's carbonyl oxygen, and the carbonyl oxygen adjacent to that donor amine is an H-bond acceptor to yet another ligand. The result is a chain of stacked, planar complexes running along one axis of the crystal.

The electronic spectrum of Ni(*trans*-14N4O<sub>2</sub>H<sub>2</sub>) H<sub>2</sub>O in water is shown in **Figure 90**. Two absorption maxima are observed, a shoulder at  $\lambda_{\text{max}} = 439 \text{ nm}$  ( $\epsilon = 60 \text{ M}^{-1} \text{ cm}^{-1}$ ) and  $\lambda_{\text{max}} = 497 \text{ nm}$  ( $\epsilon = 90 \text{ M}^{-1} \text{ cm}^{-1}$ ). Generally, only a single absorption

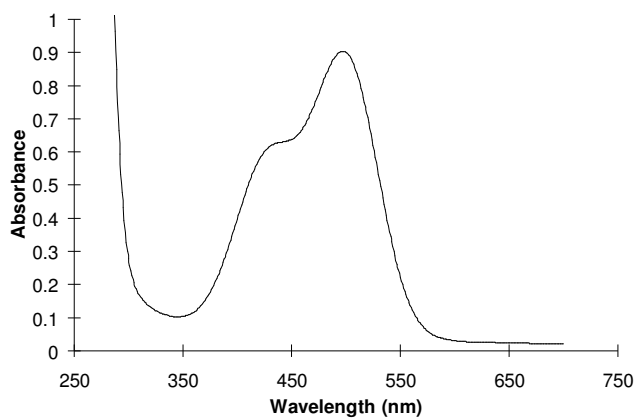


**Figure 90.** Electronic spectrum of 0.01 M Ni(*trans*-14N4O<sub>2</sub>H<sub>2</sub>) in water

band is observed for low spin, square planar Ni<sup>2+</sup> complexes.<sup>165</sup> In the 12-membered dioxocyclam, **4**, (**Figure 87**), however, a spectrum having two maxima was observed, while in the 13-15 membered *cis*-dioxomacrocycles, (**Figure 87**), only single absorption bands are seen in the range

410-465 nm.<sup>204</sup> These single bands, and the lowest energy band for the complex of the 12-membered ligand, have been assigned as the xy polarized absorption band arising from the low spin, square planar Ni<sup>2+</sup> species and its

energy is taken as the ligand field strength  $Dq_{xy}$ . In the 12-membered ligand case, the higher energy band was attributed to the coexistence of an octahedral structure probably having the macrocycle occupying all equatorial positions in the *trans* geometry, since folding of the dioxo-ligand was expected to be energetically unfavorable. Equilibria between these two forms are common in coordinating solvents for many  $Ni^{2+}$  complexes with tetraazamacrocycles,<sup>205</sup> Such spin-state equilibria are not common for complexes of di-oxo ligands. It is interesting that the equilibrium has been reported for the system containing the 12 membered ligand that also has the amidate donors *trans* to each other and also has the lowest energy absorption for the square planar form at 465 nm. If a similar assignment of the two bands is made in the present case, the square planar band would be at 497 nm ( $Dq_{xy} = 20,100 \text{ cm}^{-1}$ ), much lower than for the 12-membered ligand ( $Dq_{xy} = 21,500 \text{ cm}^{-1}$ ), and again an equilibrium is present in which some octahedral complex appears to be present (shoulder at 439 nm). These observations indicate that the ligand field strength of *trans*-14N4O<sub>2</sub>H<sub>2</sub> with  $Ni^{2+}$  is not as strong as that for the *cis*-dioxocyclam ligand ( $Dq_{xy} = 21,740 \text{ cm}^{-1}$ ).<sup>204</sup> Since the same donor types and numbers and planar coordination geometry are present in both cases, it is unclear why such a large

difference in ligand field strength occurs.

The cyclic voltammogram of  $Ni(\textit{trans}\text{-}14N4O_2H_2)$  in water is presented in **Figure 91**. The oxidation to  $Ni^{3+}$  is found at  $E_{ox} = +0.964 \text{ V}$  (vs SHE), but is not reversible, with  $\Delta E \sim 450 \text{ mV}$ . For comparison, the  $Ni^{3+}/Ni^{2+}$   $E_{1/2}$  values for macrocycles **1-4** (*cis*

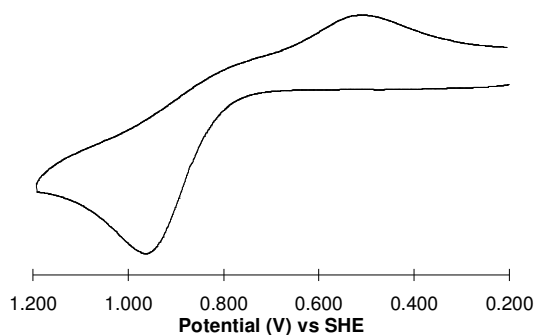


**Figure 91.** Cyclic voltammogram of  $Ni(\textit{trans}\text{-}14N4O_2H_2)$  in water

oxo location in 13-15 membered cases) are: Ni(**4**) = +0.86V, Ni(**1**) = +1.16V, Ni(**2**) = +1.04V, Ni(**3**) = +0.86.<sup>200</sup> The one electron oxidation of Ni(*trans*-14N4O<sub>2</sub>H<sub>2</sub>) is quite similar to the other complexes in potential, although the other complexes generally are much more reversible. Again, the origin of the difference in electrochemical behavior is not known, since the same donor atoms and geometry seem to be in place for both the *cis* and *trans* dioxo ligands. Perhaps locating the rigidifying amidate groups *trans* to one another modifies the ring's ability to adjust to the smaller Ni<sup>3+</sup> cation produced upon one electron oxidation, resulting in a species with a much larger geometry difference with the Ni<sup>2+</sup> precursor than is the case for the *cis*-dioxo ligands.

### Cu<sup>+</sup> and Cu<sup>2+</sup> Complexes of Bn<sub>2</sub>B14N4

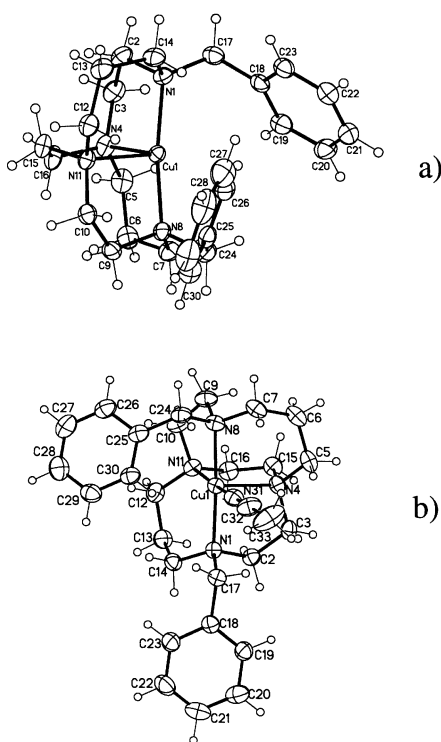


**Figure 92.** Molecular structures of a) Cu(Bn<sub>2</sub>B14N4)<sup>+</sup> and b) Cu(Bn<sub>2</sub>B14N4)(MeCN)<sup>2+</sup>

To further investigate the properties of the interesting ethylene cross-bridged ligands, the copper(I) complex of a benzyl disubstituted cross-bridged cyclam, Bn<sub>2</sub>B14N4 was prepared and examined by X-ray crystallography. The Cu<sup>+</sup> ion was found to coordinate to all four tertiary nitrogens of the bicyclic ligand, in what is best described as an extremely distorted tetrahedral geometry (**Figure 92a**, **Table 31**). The preferred coordination

**Table 31.** Selected bond lengths (Å) and angles (°) for copper-Bn<sub>2</sub>B14N4 complexes

(i) For <b>Cu(Bn<sub>2</sub>B14N4)<sup>+</sup></b>			
Cu(1)-N(8)	2.0105(13)	Cu(1)-N(4)	2.1608(13)
Cu(1)-N(1)	2.0204(13)	Cu(1)-N(11)	2.1715(13)
N(8)-Cu(1)-N(1)	171.85(5)	N(8)-Cu(1)-N(11)	89.04(5)
N(8)-Cu(1)-N(4)	97.96(5)	N(1)-Cu(1)-N(11)	96.92(5)
N(1)-Cu(1)-N(4)	88.12(5)	N(4)-Cu(1)-N(11)	85.17(5)
(ii) For <b>Cu(Bn<sub>2</sub>B14N4)(MeCN)<sup>2+</sup></b>			
Cu1-N31	2.048(3)	Cu1-N1	2.116(2)
Cu1-N8	2.056(2)	Cu1-N4	2.142(2)
Cu1-N11	2.087(2)		
N31-Cu1-N8	88.17(10)	N11-Cu1-N1	93.34(9)
N31-Cu1-N11	173.05(10)	N31-Cu1-N4	97.76(10)
N8-Cu1-N11	86.29(10)	N8-Cu1-N4	95.29(10)
N31-Cu1-N1	91.99(9)	N11-Cu1-N4	86.94(9)
N8-Cu1-N1	177.34(10)	N1-Cu1-N4	87.32(9)

geometry of the d<sup>10</sup> metal ion would be tetrahedral, but the ligand cavity is not large enough to provide this environment undistorted. The Cu<sup>+</sup> ion has one very large bond angle, N(8)-Cu(1)-N(1) = 171.85(5)°, that demonstrates the magnitude of the distortion.

The other N-Cu-N bond angles are all much smaller, from 85.17(5)-97.96(5)°. The N(1)-Cu(1) = 2.0204(13) Å and N(8)-Cu(1) = 2.0105(13) Å bond lengths are also quite short compared to the other Cu-N bond length of N(4)-Cu(1) = 2.1608 Å and N(11)-Cu(1) = 2.1715 Å and to the average four coordinate copper(I) to tertiary nitrogen bond length of 2.139 Å.<sup>206</sup> This short bond length indicates how difficult it is for the ligand cavity to accommodate Cu<sup>+</sup> in something approaching its preferred tetrahedral geometry. Finally, it should be noted, that this is the first structure of an ethylene cross-bridged cyclam in which the metal ion is completely enclosed within the ligand cavity (the ~172° bond angle is bent into the cavity) as opposed to the many other structures (*vide supra*) with this size of cross-bridged ligand and other, smaller metal ions, such as Mn<sup>2+</sup>, Fe<sup>2+</sup>, Co<sup>2+</sup>, Ni<sup>2+</sup>, Zn<sup>2+</sup>, Mn<sup>3+</sup>, and Fe<sup>3+</sup>, which find the metal ion extending out somewhat from the ligand cavity (axial N-M-N bond angles < 180° bent away from the ligand cavity). It is proposed that the metal ions' geometric preference forces this occurrence.

The product of air oxidation of Cu(Bn<sub>2</sub>B14N4)<sup>+</sup> in acetonitrile is the green Cu<sup>2+</sup> complex of the unmodified ligand in which an acetonitrile molecule is now the fifth ligand (**Figure 92b, Table 31**). This complex is similar to previous Cu<sup>2+</sup>

complexes of ethylene cross-bridged ligands, which tend to have square pyramidal coordination geometries, as is the present case. Here the acetonitrile ligand and three of the macrobicycle nitrogens are the equatorial ligands, with one bridgehead nitrogen of the ligand acting as the axial ligand. The flexibility of the benzyl groups of this ligand are demonstrated in this structure as one must rotate to fold away from the copper(II) ion, in order for the acetonitrile ligand to coordinate. In the  $\text{Cu}^+$  complex, both benzyl groups are folded towards the metal ion, essentially occupying the empty fifth coordination site. Again, this complex has the metal ion completely engulfed, though less so with the N(1)-Cu(1)-N(8) bond angle now at  $177.34(9)^\circ$ , but with this angle still bent into the ligand cavity.

### The Square Pyramidal $\text{Pd}^{2+}$ Complex of B14N4

The coordination geometries of complexes of  $\text{Pd}^{2+}$ , as with other transition metal ions, result from a delicate interplay between ligand-field favorability for the metal ion and the steric and topological constraints of the ligand(s).<sup>3,158</sup> As a  $d^8$  ion,  $\text{Pd}^{2+}$  is overwhelmingly found in four-coordinate square planar complexes, to maximize occupation of bonding orbitals.<sup>8</sup> Geometries other than square planar for

$\text{Pd}^{2+}$  are observed only when the steric or topological demands of the ligand outweigh the loss in stabilization due to the geometric distortion.

$\text{Pd}(\text{B14N4})\text{Cl}^+$  (**Figure 93**, **Table 32**) exhibits such a distorted geometry, in this case a five-coordinate square pyramidal one, because the short ethylene cross-bridge of the macrocyclic ligand B14N4 does not

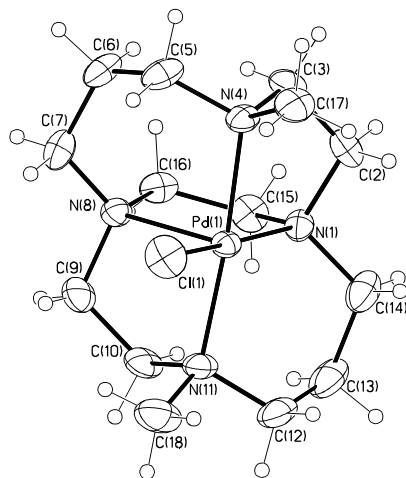


**Figure 93.** Molecular structure of  $\text{Pd}(\text{Me}_2\text{B14N4})\text{Cl}^+$

allow the macrocycle to occupy the four sites of a square plane. The topological constraint of the two-carbon bridge enforces a fold in the ligand that is conserved on binding to Pd<sup>2+</sup>.

The only non-adjacent nitrogen pair capable of spanning the diagonal of the square pyramid's base, N4 and N11, do so, giving N(4)-Pd-N(11) = 171.64(11). The

**Table 32.** Selected bond lengths (Å) and angles (°) for **Pd(Me<sub>2</sub>B14N4)Cl<sup>+</sup>** single chloride ligand completes the coordination sphere of Pd<sup>2+</sup>, and allows the complex to retain part of the advantage

Pd(1)-N(4)	2.078(3)	Pd(1)-Cl(1)	2.3407(10)
Pd(1)-N(11)	2.101(3)	Pd(1)-N(8)	2.461(3)
Pd(1)-N(1)	2.112(3)		
N(4)-Pd(1)-N(11)	171.65(11)	N(1)-Pd(1)-Cl(1)	169.68(8)
N(4)-Pd(1)-N(1)	85.07(12)	N(4)-Pd(1)-N(8)	89.61(10)
N(11)-Pd(1)-N(1)	91.00(12)	N(11)-Pd(1)-N(8)	82.45(10)
N(4)-Pd(1)-Cl(1)	89.87(9)	N(1)-Pd(1)-N(8)	80.12(10)
N(11)-Pd(1)-Cl(1)	95.12(9)	Cl(1)-Pd(1)-N(8)	108.89(7)

of a square-based geometry. The chemically equivalent nitrogens, N(1) and N(8), occupy inequivalent sites on the square pyramid; N(1) is on the base while N(8) is at the apex. This inequality is evident in the Pd-N distances: Pd-N(1) = 2.112(3) Å while Pd-N(8) is 2.461(3) Å. The long Pd-N(8) bond demonstrates that ligand topology dictates the coordination geometry in this complex, rather than it being determined by the electronic configuration of the Pd<sup>2+</sup> ion as in less topologically constrained ligand complexes. The result of the mismatch between ligand constraints and metal ion ligand field effects, is a rather unsymmetric complex where only chloride and an "empty" site (of an octahedron) occupy one hemisphere of the palladium ion, while the entire bicyclic ligand is in the other hemisphere.

### A Cyclam-like Macrocycle Side-Bridged by a Propyl Chain

The compound *meso*-5,5,7,12,12,14-hexamethyl-1,4,8,11-tetraazabicyclo[9.3.3]heptadecane, was synthesized during the study of the transition metal complexes of cross-bridged tetraazamacrocycles. Generally, ethylene bridges across non-adjacent nitrogens of tetraazamacrocycles are obtained by their condensation with glyoxal,

selective alkylation at two non-adjacent nitrogens, and finally, ring-opening reduction of the diquat intermediate.<sup>113</sup> However, substituted macrocycles, like *meso*-14N4Me<sub>6</sub> are more difficult to bridge by this route because of the added steric bulk of the six C-methyls (*vide supra*).

Another route was explored to the cross-bridged analogue of *meso*-14N4Me<sub>6</sub> based on the successful trans-dialkylation of *meso*-14N4Me<sub>6</sub> in which the geminal dimethyl groups apparently sterically protect two of the macrocycles four secondary amines from reaction.<sup>207</sup> 1,3-diiodopropane was chosen as the bis-electrophile in the bridging reaction because 1,2-dihaloethanes have been shown to preferentially bridge adjacent nitrogens of tetraazamacrocycles giving the stable piperazine derivatives, which were unwanted.<sup>39</sup> Rather than the expected cross-bridged product, *meso*-

5,5,7,12,12,14-hexamethyl-1,4,8,11-tetraazabicyclo[9.3.3]heptadecane

(**Figure 94**), in which the trimethylene group had bridged adjacent nitrogens N4 and N8, was isolated giving an eight-membered ring as part of the bicyclic product.

Its structure also revealed that it was diprotonated at nitrogens N1 and N8; counterions of iodide and chloride (apparently originating in

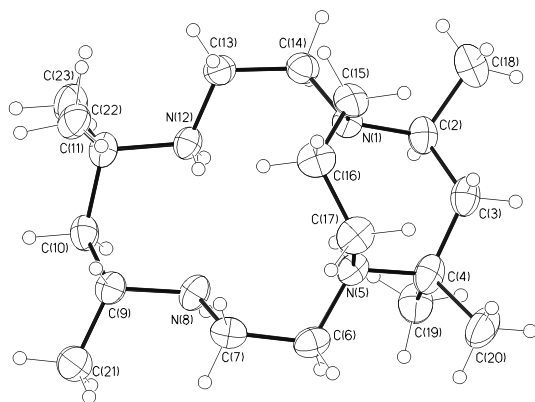


**Figure 94.** Molecular structure of H<sub>2</sub>(*meso*-5,5,7,12,12,14-hexamethyl-1,4,8,11-tetraazabicyclo[9.3.3]heptadecane)<sup>2+</sup>

chloroform used during the synthesis) and an ether of crystallization complete the salt.

No other side-bridged fourteen-membered tetraazamacrocycles have been structurally characterized that locate the side bridge across two nitrogens separated by three carbons in the starting macrocycle. The trimethylene bridging group seems to fit the geometry of the already present trimethylene bridge between N4 and N8 giving

the eight-membered ring in preference to the cross-bridged product regardless of the steric bulk of the geminal dimethyl group  $\alpha$  to N4, which prohibits alkylation by non-bridging groups.<sup>207</sup>